

Neutron Scattering Study of Quantum Phase Transitions in Integral Spin Chains.

A. Zheludev

Condensed Matter Sciences Division, Oak Ridge National Laboratory, Oak Ridge, TN 37831-6393, USA.

Abstract. Quite a few low-dimensional magnets are quantum-disordered “spin liquids” with a characteristic gap in the magnetic excitation spectrum. Among these are antiferromagnetic chains of integer quantum spins. Their generic feature are long-lived massive (gapped) excitations (magnons) that are subject to Zeeman splitting in external magnetic fields. The gap in one of the magnon branches decreases with field, driving a soft-mode quantum phase transition. The system then enters a qualitatively new high-field phase. The actual properties at high fields, particularly the spin dynamics, critically depend on the system under consideration. Recent neutron scattering studies of organometallic polymer crystals NDMAP (Haldane spin chains with anisotropy) and NTENP (dimerized $S = 1$ chains) revealed rich and unique physics.

INTRODUCTION

A quarter of a century ago the interest in quantum magnetism was rekindled by the famous work of Haldane [1], who showed that integer-spin one-dimensional (1D) Heisenberg antiferromagnets (AFs) have a non-degenerate ground state and an energy gap in the excitation spectrum. Quantum zero-point fluctuations are so strong that the spin correlation function decays exponentially, and these systems can be viewed as 1D “spin liquids”. Their properties are in stark contrast with those of half-integer spin chains that are gapless, and where spin correlations decay according to a slow power-law (Luttinger spin liquids).

Haldane spin chains have been studied extensively, and are by now very well understood. The exact ground state is not known, but is similar to the easy to visualize Valence Bond Solid (VBS) state [2]. The latter is constructed by representing each $S = 1$ spin as two separate $S = 1/2$ spins, binding pairs of these into antiferromagnetic dimers for each exchange bond, and projecting the resulting state back onto the subspace where $S_i^2 = 2$ on each site, as schematically shown in the insets on the left side Fig. 1. Each exchange link carries exactly one valence bond, and the periodicity of the underlying crystal lattice remains intact. Considerably less attention has been given to a *different* quantum spin liquid that is realized in $S = 1$ AF spin chains with exchange interactions of alternating strength. As the alternation parameter $\delta = (J_1 - J_2)/(J_1 + J_2)$ deviates from zero, the energy gap Δ decreases and closes at some critical value $|\delta| = \delta_c \approx 0.26$ [3, 4, 5, 6]. Increasing $|\delta|$ beyond this quantum-critical point re-opens the spin gap. The ground

state is then no longer the Haldane state, but a dimerized one. The corresponding valence bond wave function is shown in right inset in Fig. 1. It contains two valence bonds on each strong link and none on the weaker ones.

The two gapped quantum phases differ by their “hidden” spin correlations [7, 4]. The Haldane state has a non-vanishing AF string order parameter [8] related to a breaking of a non-local $Z_2 \times Z_2$ symmetry [7]. The highly non-local multi-spin correlation function that defines AF strings can not be expressed through the usual pair spin correlation functions $\langle S_i(0)S_j(t) \rangle$, that contribute to the dynamic susceptibility $\chi(\mathbf{q}, \omega)$. As a result, string order can not be directly observed experimentally.

Qualitatively new physics is expected to emerge in strong magnetic fields. Since the lowest-energy gap excitations are a $S = 1$ triplet, they are subject to Zeeman splitting. With increasing field gap in one of the three modes decreases and eventually vanishes, leading to a 1-D Bose condensation of magnons [9, 10, 11, 12]. A qualitatively new state emerges at higher fields. For isotropic or XY-like spin chains (axial symmetry) theory predicts an extended quantum-critical state with power-law spin correlations and certain incommensurate features [13, 11, 14, 12, 15, 16]. However, in the presence of magnetic anisotropy the high-field state is magnetically ordered at $T = 0$: a *uniform* external field suppresses quantum spin fluctuations and induces *staggered* (AF) long-range order [13, 11]. Even in the ordered state quantum effects are significant, and the system is a “quantum spin solid”. Schematic phase diagrams for the axially symmetric and asymmetric cases are shown in Fig. 1.

Field-induced condensation of magnons and long-range ordering was studied in a number of quantum-

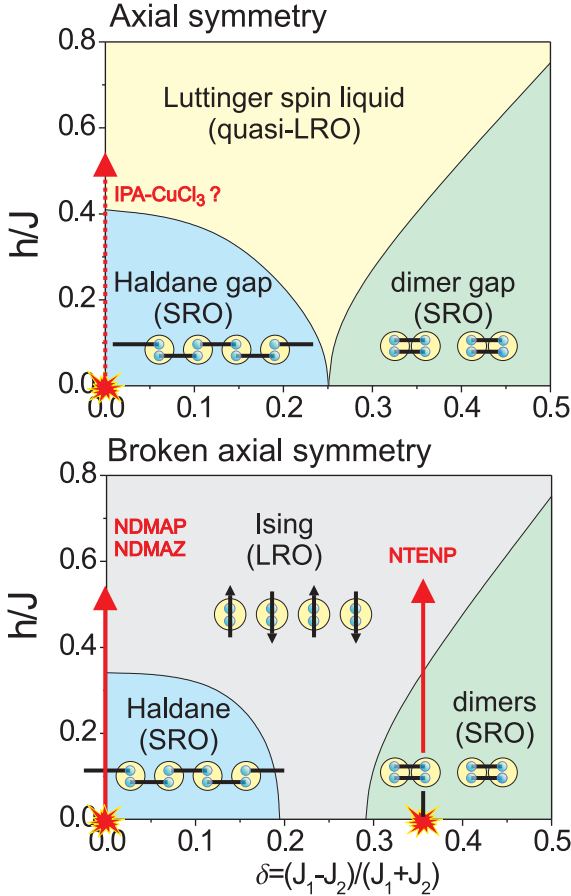


FIGURE 1. Schematic phase diagrams of bond-alternating $S = 1$ chains in external magnetic fields for axially symmetric (top) and axially asymmetric (bottom) models.

disordered gapped spin systems. The best known examples are those of the spin-Peierls material CuGeO_3 [17], the $S = 1/2$ Shastry-Sutherland lattice $\text{SrCu}_2(\text{BO}_3)_2$ [18, 19] and the dimer compound TlCuCl_3 [20]. None of these materials realize the $S = 1$ model, and all fall far from being ideal 1D magnets. Moreover, for CuGeO_3 [17] and $\text{SrCu}_2(\text{BO}_3)_2$ [21] the physics is complicated by the involvement of the crystal lattice. The present review is focused on a plain Heisenberg $S = 1$ chain, where it is the integrity of spin and the non-trivial topology of one dimension that conspire to produce spectacular and exotic behavior in high fields. The central question that will be asked is whether Haldane-gap and dimerized $S = 1$ chains behave any differently when magnetized?

Excellent realizations of the $S = 1$ Heisenberg chain model can be found among Ni-based organometallic polymer crystals. In this family $\text{Ni}(\text{C}_2\text{H}_8\text{N}_2)_2\text{NO}_2(\text{ClO}_4)$ (NENP) is perhaps the one most extensively studied material [22, 23, 24, 25, 26]. Unfortunately, the magnetic Ni^{2+} ions in NENP have

a staggered g -factor [27, 28]. As a result, an external magnetic field necessarily induces an internal staggered field that ruins the phase transition. A breakthrough in the study of high-field quantum phases of $S = 1$ chains came with the recent discovery of the compounds $\text{Ni}(\text{C}_5\text{D}_{14}\text{N}_2)_2\text{N}_3(\text{PF}_6)$ (NDMAP) [29, 30, 31, 32, 33, 34, 35, 36] and $\text{Ni}(\text{C}_5\text{H}_{14}\text{N}_2)_2\text{N}_3(\text{ClO}_4)$ (NDMAZ) [37, 38], that are structurally similar to NENP, but are free of the staggered g -factor problem. An even more exciting development was the discovery of $[\text{Ni}(\text{N}, \text{N}'\text{-bis}(3\text{-aminopropyl})\text{propane-1,3-diamine}(\mu\text{-NO}_2)]\text{ClO}_4$ (NTENP) [39, 40, 41, 42], that is also structurally similar, but features bond-alternating $S = 1$ chains. In the study of high-field phenomena in NDMAP, NDMAZ and NTENP neutron scattering proved itself as the most useful experimental tool.

DIMERIZED VS. HALDANE CHAINS

Structures. The crystal structures of the Haldane-gap material NDMAP and the bond-alternating chain system NTENP are shown in Fig. 2. The key features of both are covalent chains of octahedrally coordinated Ni^{2+} ions. Only nearest-neighbor in-chain AF interactions are relevant. The coordination geometry results in a substantial single-ion magnetic anisotropy, with a magnetic easy plane that is almost perpendicular to the chain direction. The chains are held together by Van Der Waals forces, so inter-chain interactions are negligible. All Ni^{2+} sites are equivalent and there is no staggered component to the Ni^{2+} g -factor in either structure. However, in NDMAP all Ni-Ni exchange pathways along the chains are equivalent, whereas in NTENP Ni-Ni distances alternate between $d_1 = 4.28 \text{ \AA}$ and $d_2 = 4.86 \text{ \AA}$. The structure of NDMAZ is similar to that of NDMAP.

Excitations in NDMAP. Both NDMAP and NTENP have a gap in the magnetic excitation spectrum that is most prominent in inelastic neutron scattering spectra. Typical scans collected at the respective 1D AF zone-centers in both compounds are shown in Fig. 3 [43, 40]. Let us first discuss the spectrum of NDMAP. There are, in fact, three distinct gap excitations, two of which are merged into a single peak at lower energies in Fig. 3a. The three peaks correspond to the three members of the triplet of Haldane gap excitations, split by magnetic anisotropy. The upper mode is polarized perpendicular to the magnetic easy-plane, *i.e.*, almost parallel to the spin chains. The asymmetric peak shapes are due to experimental resolution that is well-characterized. The gap energies for the three modes are $\Delta_1 = 0.42(3) \text{ meV}$, $\Delta_2 = 0.52(6) \text{ meV}$, and $\Delta_3 = 1.9(1) \text{ meV}$ [43]. Using known numerical results for anisotropic Haldane spin

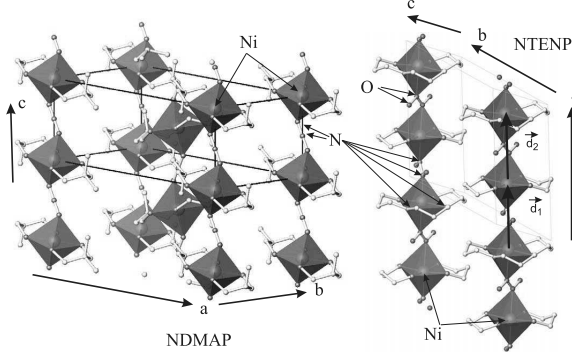


FIGURE 2. A schematic view of the uniform $S = 1$ Ni^{2+} spin chains in NDMAP and bond-alternating chains in NTENP. The equatorial vertices of the Ni^{2+} coordination octahedra are nitrogen atoms. The octahedra are coupled via azide and NO_2 groups. Oxygen and nitrogen atoms are shown as dark grey spheres. Light grey spheres are carbon atoms.

chains[44, 45] one can obtain the exchange constant $J = 2.3$ meV ($\bar{\Delta}/J = 0.41$) and the anisotropy parameter $D/J \approx 0.25$, which are in good agreement with estimates based on high-temperature susceptibility measurements [29]. The intensities of the three peaks, apart from the polarization dependence of the inelastic cross section for unpolarized neutrons, scale almost exactly as $1/\omega$.

Ground state of NTENP. For NTENP $J = 3.4$ meV [39], based on high-temperature measurements. Using the measured gap energies $\Delta_1 = 0.42(3)$ meV, $\Delta_2 = 0.52(6)$ meV, and $\Delta_3 = 1.9(1)$ meV one gets $\bar{\Delta}/J = 0.4$, i.e., which is almost exactly the same ratio as for a uniform spin chain [40, 41]. Does NTENP then have a Haldane ground state with very little alternation of exchange interactions, or does the gap instead originate from dimerization, with $\bar{\Delta}/J \approx 0.4$ being just a coincidence? Deciding which is the case is not trivial, since the only qualitative distinction between the two possible ground states is the elusive and unmeasurable string order parameter. Yet, one can look for quantitative differences. For example, following the dispersion of magnons in NTENP gives a measure of the zone-boundary energy $\hbar\omega_{\text{ZB}}/J = 2.2$ [40, 42]. This value is smaller than that for a Haldane spin chain where $\hbar\omega_{\text{ZB}}/J = 2.7$ [46]. In fact, recent numerical work [47] directly relates $\hbar\omega_{\text{ZB}}/J$ to δ and allows to estimate $\delta \approx 0.3$ for NTENP. Thus, NTENP is indeed strongly dimerized and is *not* in a Haldane ground state.

Inelastic neutron scattering actually provides a tool for directly measuring the level of dimerization in a bond-alternating chain. Applying the Hohenberg-Brickman sum rule [48] for the first moment of the dynamic struc-

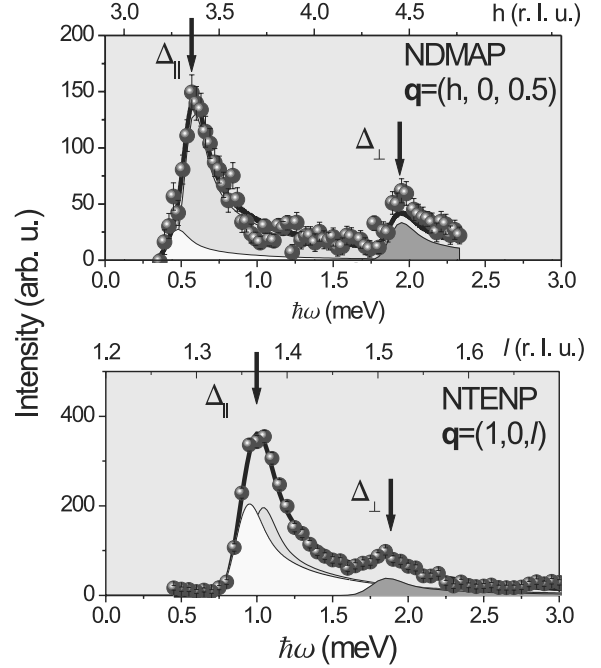


FIGURE 3. Typical neutron spectra collected for the Haldane-gap material NDMAP (top) and the $S = 1$ dimer-gap system NTENP (bottom) at the respective 1D antiferromagnetic zone-centers. NDMAP and NTENP data are from refs. [43] and [35], respectively.

ture factor of a bond-alternating spin chain one gets:

$$\int_{-\infty}^{\infty} (\hbar\omega) S^{\alpha\alpha}(\mathbf{q}, \omega) d(\hbar\omega) = -\frac{4}{3}E_1 \sin^2(\mathbf{q}\mathbf{d}_1/2) - \frac{4}{3}E_2 \sin^2(\mathbf{q}\mathbf{d}_2/2). \quad (1)$$

Here \mathbf{d}_1 and \mathbf{d}_2 are real-space vectors chosen along the short and long bonds in the chains. The quantities $E_1 = J_1 \langle \mathbf{S}_{2j} \mathbf{S}_{2j+1} \rangle$ and $E_2 = J_2 \langle \mathbf{S}_{2j} \mathbf{S}_{2j-1} \rangle$ are ground state *exchange energies* associated with the strong and weak bonds, respectively. Thus, by measuring the energy-integrated intensities of magnetic excitations in different Brillouin zones, it was possible to directly extract the modulation of exchange energy $\delta' = \frac{E_1 - E_2}{E_1 + E_2} \approx 0.42$ for NTENP [40]. Numerical calculations were then used to obtain δ from δ' , reaching the same conclusion: NTENP is strongly dimerized. Based on a combination of techniques it was concluded that for NTENP $J_1 = 2.2$ meV, $J_2 = 4.7$ meV and $D \approx 0.3$ meV.

Excitations in NTENP. Let us now return to the spectrum measured in NTENP at the 1D AF zone center and shown in Fig. 3b. After correcting for the usual polarization factors, it was found that the intensity of the higher-energy gap mode ($\Delta = 1.9$ meV) in NTENP is anomalously small: at least 4 times weaker than expected from

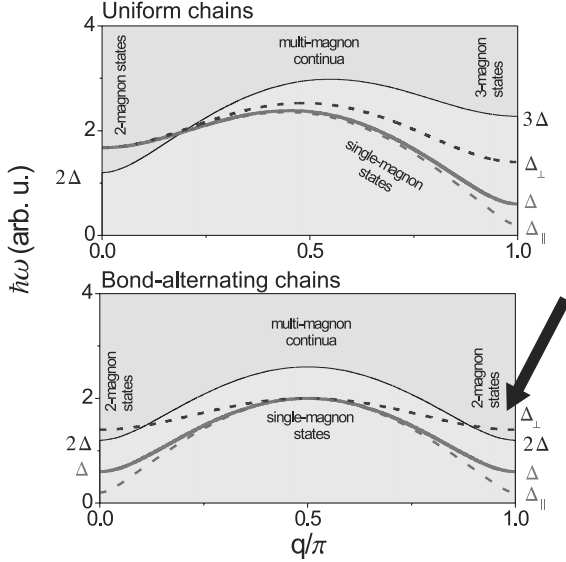


FIGURE 4. A simplified view of the excitation spectra in uniform (top) and bond-alternating (bottom) quantum $S = 1$ chains. Lines are as explained in the text.

the usual $1/\omega$ scaling typical of antiferromagnets and obeyed very well in NDMAP. The physical significance of this observation was recently revealed in numerical calculations of the excitation spectrum performed using realistic exchange and anisotropy parameters [42, 49]. It was shown that in NTENP, unlike in NDMAP, for the higher-energy-mode there is an open channel of decay into a pair of lower-energy gap modes. This decay process leads to a downward renormalization of the upper mode's intensity and gives it a finite lifetime (energy width). An equivalent interpretation is that the upper mode occurs in the $E - \mathbf{q}$ range occupied by a continuum of 2-magnon excitations. In NTENP the observed upper mode is very close to the lower continuum bound.

The key to understanding this difference in behavior is the breaking of translational symmetry in bond-alternating spin chains. Figure 4 schematically shows the spectra for the uniform and bond-alternating cases. In both systems the lowest-energy excitation near $q = \pi$ are a triplet of long-lived gap excitations at an energy Δ . These are shown in heavy solid lines, with the assumption that no magnetic anisotropy is present. In a Haldane spin chain the single-magnon energy becomes rather large near $q = 0$, the spectrum resembling that of a spin ladder [50]. As a result, the lowest-energy excitations near $q = 0$ are actually a continuum of 2-magnon states with a gap of roughly 2Δ [51]. Not so in a bond-alternating spin chain where $q = 0$ and $q = \pi$ are *equivalent* due to symmetry breaking. Here the dispersion resembles that of coupled $S = 1/2$ dimers and the magnon triplet at $q = 0$ again has a gap of Δ . Returning to $q = \pi$, we see that in

a Haldane chain the lowest-energy excitations above the magnons are 3-magnon states, starting at a rather high energy of 3Δ [52]. In a bond-alternating chain at $q = \pi$ 2-magnon states are allowed, so the continuum starts at a lower energy of 2Δ . If the magnon branches become split by anisotropy, as is the case for NDMAP and NTENP, the upper (out-of-plane) mode at $q = \pi$ moves upwards towards the lower continuum bound. This is illustrated by dashed lines in Fig. 4. The lower bounds of the continua actually moves down in the anisotropic case (not shown). In NTENP the upper mode thus becomes submerged in the low-lying 2-magnon continuum and can decay into a pair of in-plane magnons. In NDMAP the continuum gap is larger to begin with, so the upper mode remains safely below it. Due to limitation on experimental resolution, the continua can not be clearly identifies, but the effect on the intensity of the upper mode is easily detected.

HIGH FIELDS

Zeeman splitting. Since the gap excitations are an $S = 1$ triplet, an external magnetic field modifies their energies by virtue of Zeeman effect. Figure 5 shows the measured field dependencies of the gaps in NDMAP and NTENP. Below H_c this behavior remarkably well accounted for by simple perturbation theory [53, 24], that considers a 2-nd order mixing induced between the excited states by the Zeeman term. In the presence of anisotropy the ground state is also affected, but only in the next order [24], so the effect on the gap energy is minimal. H_c obtained from perturbation theory is very close to the actual observed value [31, 38, 36, 42]. More sophisticated theoretical models can achieve an even better agreement with experiment [33, 35, 34].

For NDMAP the upper Haldane gap mode persists as a well-defined sharp excitation all the way to H_c and beyond (see Fig. 8). In contrast, in NTENP, where the upper mode is anomalously weak already at $H = 0$, it further weakens and then totally vanishes well below the transition. This is illustrated in Fig. 6 and Fig. 9 that show data from [42]. Such behavior is easy to understand within the hand-waving picture presented in the previous section. With increasing H the upper mode moves further into the 2-magnon continuum, while the lower bound of the continuum actually moves down. A larger portion of the 2-particle phase space becomes available for final decay state of magnons from the upper branch, which further affects their width and intensity.

Field-induced spin freezing. Once the gap in the lower mode is driven to zero, the gapped quantum spin liquid “freezes”. All high-field experiments on NDMAP, NDMAZ and NTENP realize the axially asymmetric

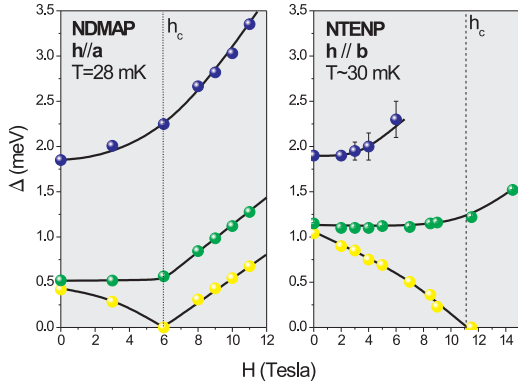


FIGURE 5. Symbols: measured field dependencies of the gap energies in NDMAP (left, Ref. [33]) and NTENP (right, Ref. [42]). Lines are guides for the eye.

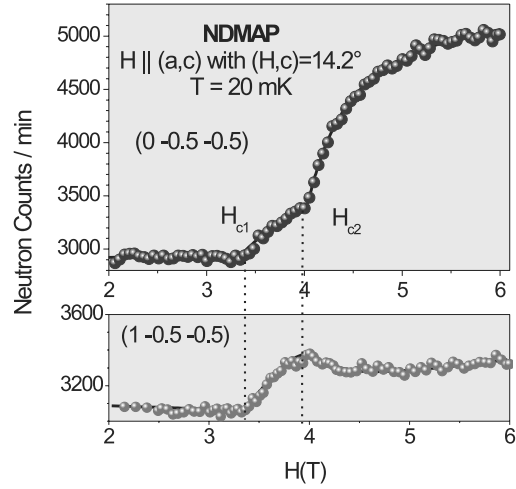


FIGURE 7. Field dependence of two magnetic Bragg reflections in NDMAP for a field applied at an angle 14° to the major crystal axes. Two consecutive spin-freezing transitions are apparent. The data are from Ref. [36].

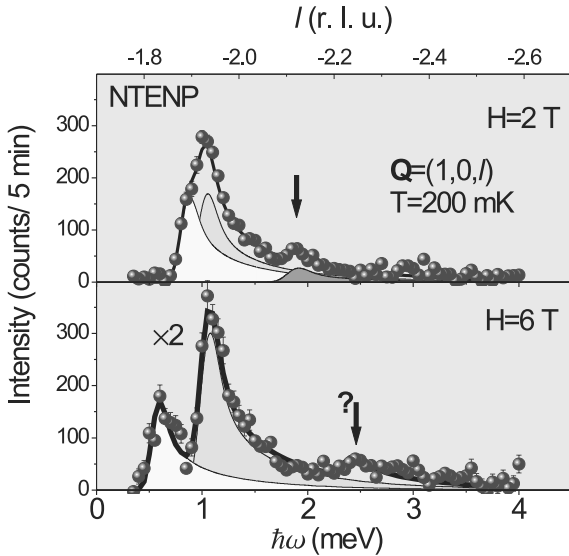


FIGURE 6. Evolution of the excitation spectrum in NTENP at the 1D AF zone-center in moderate applied fields. Zeeman splitting of the lower excitation doublet is apparent. The upper mode progressively weakens and broadens. It is no longer observable above 6 T. The data are from Ref. [42].

geometry in which above the critical field even an isolated chain has antiferromagnetic long-range order at $T = 0$. Weak inter-chain interactions stabilize this long-range order at non-zero temperatures [54]. A signature of this field-induced antiferromagnetism is the appearance of new Bragg reflections at $H > H_c$. Such reflections were observed by means of neutron diffraction in NDMAP [31, 36], NDMAZ [38] and NTENP [42], and the approximate structures of the high-fielded phases

were determined. In all cases the ordered staggered moment lies perpendicular to the direction of applied field and within the magnetic easy-plane. This spin arrangement allows the system to become magnetized: the ordered moments canttilt slightly in the direction of the field, to produce a net uniform magnetization. Interestingly, a relatively small field in excess of H_c can produce a large staggered moment. For example, in NDMAP, where $H_c = 4.5$ T, in magnetic fields of 7 T the sublattice magnetization is already as high as $1.2 \mu_B$ per site.

As far as static properties are concerned, there are no qualitative differences between magnetized Haldane versus dimerized spin chains. Nevertheless, two peculiarities of spin freezing in NDMAP are worth mentioning. First of all, in NDMAP there are two sets of AF $S = 1$ chains that are totally decoupled due to geometric frustration of exchange interactions. The local anisotropy axes of all magnetic ions tilted by $\alpha = 16^\circ$ relative to the crystal c axis. The tilt directions are *opposite* for spins belonging to the two different sets of chains. As a result, when the field is applied in a direction other than along the principal crystallographic axes, the angles between local anisotropy axes and field are *different* for the two sets of chains. Spin freezing then occurs first only in one set of chains at a critical field H_{c1} . The other chains remain gapped and disordered up to a second critical field $H_{c2} > H_{c1}$, at which they will also order. This two-stage spin freezing results in a peculiar field dependence of magnetic Bragg intensities as shown in Fig. 7, and explained in detail in Ref. [36].

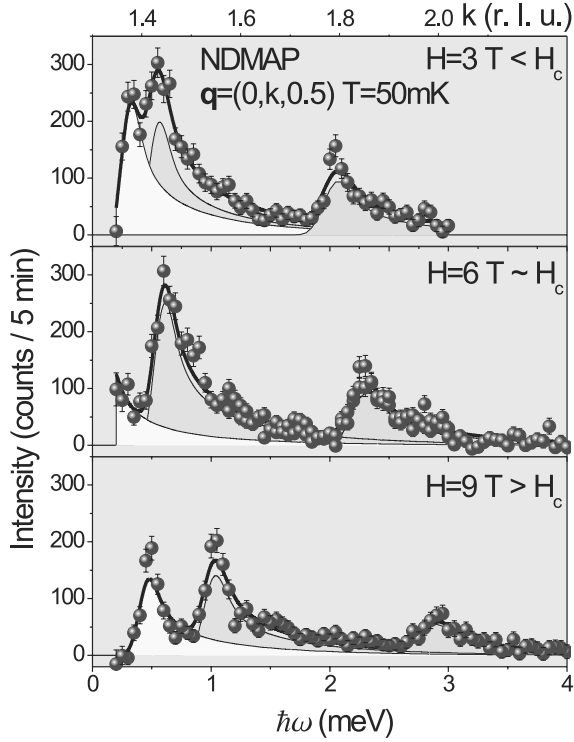


FIGURE 8. Evolution of the excitation spectrum of the Haldane-gap system NDMAP at the 1D AF zone-center upon crossing the critical field H_c . All three branches survive in the high-field ordered state. Conventional spin wave theory can account for only two transverse-polarized modes. The data are from Ref. [33].

Another interesting feature of spin freezing NDMAP is due to that non-frustrated inter-chain interactions span over at least 18\AA along the a axis. They are extremely weak and presumably of dipolar origin. As these interactions are crucial to establishing true long-range order, the degree of ordering becomes dependent on the field direction. In most geometries for NDMAP a 3D-ordered state is observed at high fields, just as for NDMAZ and NTENP. However, in experiments where the field was applied perpendicular to the chains, one instead observes *two-dimensional* spin freezing [31]. Sufficiently long-range AF spin correlations are established in layers parallel to the (b, c) plane, but such layers remain uncorrelated along the a direction. This unusual *anisotropic correlated spin glass* state is characterized by Bragg *rods* (as opposed to Bragg *peaks*) parallel to the a^* axis.

Dynamics of quantum spin solids. Even though at high fields the ground states of the Haldane gap material NDMAP and the dimerized system NTENP are characterized by long-range antiferromagnetic order as in “conventional” magnets, their excitation spectra are *nothing*

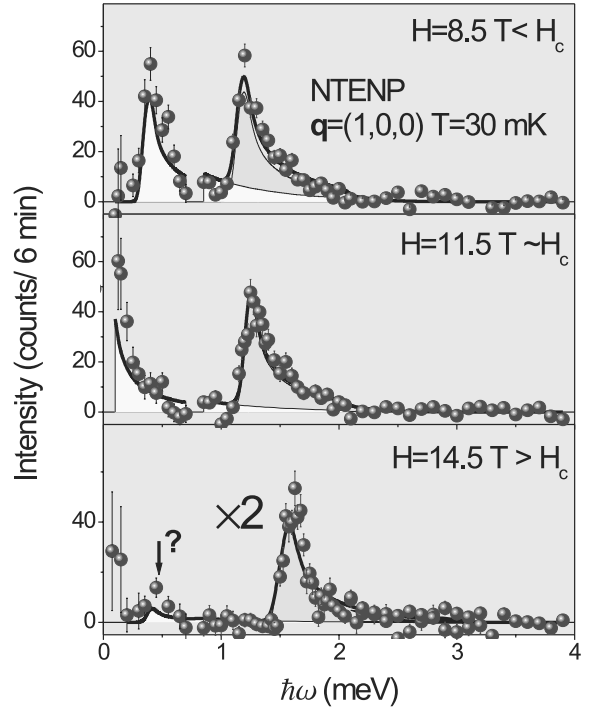


FIGURE 9. Evolution of the excitation spectrum of the $S = 1$ dimerized system NTENP at the 1D AF zone-center upon crossing the critical field H_c . Unlike in NDMAP, only one excitation branch survives in an intense sharp excitation in the high-field ordered state. The data are from Ref. [42].

like that predicted by semiclassical spin wave theory (SWT). Figures 8 and 9 are a comparison of energy scans measured at the 1D AF zone-centers in NDMAP in NTENP at 3 T below the critical field, almost exactly at the quantum phase transition point, and at 3 T above.

The most striking feature of the spectrum of NDMAP is the persistence of *three* sharp gaps above H_c [33, 35]. The gap in the lower mode closes at the transition point but promptly re-opens in higher fields. SWT can account for only *two* excitation branches. Indeed, conventional spin waves represent a precession of the ordered moments around their equilibrium orientation (z axis), and are thus necessarily polarized in the *transverse* direction. Two independent precessions, with $S_z = \pm 1$ are all there is. In NDMAP the polarizations of magnetic excitations above the critical field have not been identified to date. Nevertheless, it is clear that one of the three branches must be a *longitudinal* mode with $S_z = 0$, representing fluctuation of the *magnitude* of the ordered moment. Where SWT is fully inadequate, a number of 1D field-theoretical models work rather well. These are typically based on mappings of the original Heisenberg Hamiltonian with anisotropy onto the quantum nonlinear σ -model, its descendent the so-called ϕ^4 -model

[11, 14, 28], Majorana fermions [13, 55], or certain dimer models [33, 34, 35]. It is important to emphasize that the re-opening of the gap in all cases is a *direct consequence* of the breaking of axial symmetry by a combination of easy-plane and in-plane anisotropies, or by the field configuration in particular experiments. In the axially symmetric case one expects a gapless high-field phase.

The high-field excitation spectrum in NTENP is qualitatively different from that in NDMAP. As can be seen in Fig. 9, in the dimerized system there is only *one* distinct long-lived excitation above H_c , a descendant of middle member of the original triplet at $H = 0$. At low energies, where in NDMAP one sees a new gap excitation, in NTENP there is very little scattering at $H > H_c$. Scans in different Brillouin zones confirm that the effect is not due to experimental polarization selectivity. A clue to what is going on is again found in numerical simulations for NTENP [42, 49]. It appears that above H_c not just the upper mode, but also the lowest-energy excitations are actually diffuse multi-magnon continua, rather than sharp single-magnon states. A very recent study [56] confirmed this picture and detected both continua.

Are the striking differences in the high-field spin dynamics of NTENP and NDMAP related to the different nature of their ground states? In answering this question the future development of analytical models for dimerized integral spin chains will be very helpful.

NEW DIRECTIONS

Breakdown of the single-mode approximation. Experiments on NTENP have demonstrated that even in the long-wavelength limit (near the 1D AF zone-center), long-lived single-particle excitations are only part of the story. Excitations with short lifetimes and entire diffuse excitation continua may constitute a substantial or even dominant fraction of the total spectral weight. Recent theoretical work [55] predicts that in Haldane spin chains one can expect similar phenomena. In particular, at some crossover field $H' < H_c$ the gap modes should become short-lived. The energy resolution of previous experiments on NDMAP was not sufficient to observe this effect. However, recent high-field neutron scattering studies on NENP contain clear evidence of broadening in at least two of the Haldane gap branches around H_c [57]. Re-investigating the excitation lifetime issue in NDMAP is clearly worthwhile.

Isotropic $S = 1$ chains. As mentioned in the introduction, the physics of the high-field phase transition in the isotropic model is expected to be totally different from that found in the strongly anisotropic NDMAP and NTENP systems. Until recently, no good model

$S = 1$ chain compounds with gap energies suitable for high field inelastic neutron scattering experiments and weak enough inter-chain interactions could be identified. A new material that seems to be almost ideal in this respect is $(\text{CH}_3)_2\text{CHNH}_3\text{CuCl}_3$ (abbreviated as IPA-CuCl₃). This compound is composed of $S = 1/2$ ladders that have *ferromagnetic* rungs, which makes them equivalent to Haldane $S = 1$ chains [58]. Anisotropy affects are negligible due to the nature of the magnetic Cu^{2+} ions. Bulk measurements revealed a field-induced Bose condensation of magnons and a quantum phase transition with $H_c \simeq 9$ T, with a remarkably isotropic $H - T$ phase diagram [59]. High field neutron scattering experiments on deuterated IPA-CuCl₃ are planned for the near future.

Incommensuration in anisotropic chains. In the presence of axial symmetry the spin correlations above H_c are expected to be incommensurate. As discussed above, in NTENP and NDMAP the magnetized phases are commensurate due to strong anisotropy effects. Only a hint of incommensurate spin correlations was detected in NDMAP, at temperatures high enough to destroy long range order [32]. Recent theories [60, 55] predict that even anisotropic models can acquire incommensurate order above some critical incommensuration field $H^* > H_c$. For NDMAP, with a field applied along the chain axis, a crude estimate yields $H^* \approx 15$ T. High-field calorimetric experiments recently discovered some sort of phase transition in NDMAP at $H \approx 14$ T [61]. It was speculated that it may be related to incommensuration. Upcoming neutron diffraction experiments will test this conjecture.

CONCLUSION

The most interesting physics is usually to be found in the *complex* behavior of *simple* model systems. Integral spin chains in external magnetic fields are a beautiful example of this.

ACKNOWLEDGMENTS

I would like to thank all those who graciously allowed me to collaborate with them on the NDMAP, NDMAZ and NTENP projects: T. Barnes (ORNL), C. Broholm (Johns-Hopkins University), Y. Chen (NIST), J. H. Chung (NIST), R. Feyerherm (HMI), B. Grenier (CEA Greoble), M. Hagiwara (Osaka University), Z. Honda (Saitame University), K. Kakurai (JAERI), K. Katsumata (RIKEN Harima Institute), Y. Koike (JAERI), A. K. Kolezhuk (Institute of Magnetism, Kiev, Ukraine), D. Mandrus (ORNL), T. Masuda (ORNL), N. Metoki

(JAERI), H.-J. Mikeska (Universität Hannover), T. Papenbrock (ORNL), S. Park (NIST), K. Prokes (HMI), Y. Qiu (NIST), L. P. Regnault (CEA Grenoble), E. Ressouche (CEA Grenoble), B. Sales (ORNL), S. M. Shapiro (BNL), A. Stunault (ILL), S. Suga (Osaka University), T. Suzuki (Osaka University), P. Vorderwisch (HMI). Work at ORNL was carried out under DOE Contract No. DE-AC05-00OR22725.

REFERENCES

1. F. D. M. Haldane, *Phys. Rev. Lett.*, **50**, 1153 (1983).
2. I. Affleck, *J. Phys.: Condens. Matter.*, **1**, 3047 (1989).
3. I. Affleck, and F. D. M. Haldane, *Phys. Rev. B*, **36**, 5291 (1987).
4. S. Yamamoto, *J. Phys. Soc. Jpn.*, **63**, 4327 (1994).
5. A. Kitazawa, K. Nomura, and K. Okamoto, *Phys. Rev. Lett.*, **76**, 4038 (1996).
6. M. T. Kohno, and M. Hagiwara, *Phys. Rev. B*, **57**, 1046 (1998).
7. T. Kennedy, and H. Tasaki, *Phys. Rev. B*, **45**, 304 (1992).
8. M. den Nijs, and K. Rommelse, *Phys. Rev. B*, **40**, 4709 (1989).
9. H. J. Schulz, *Phys. Rev. B*, **34**, 6372 (1986).
10. K. Katsumata, H. Hiroi, M. D. T. Takeuchi, A. Yamagishi, and J. P. Renard, *Phys. Rev. Lett.*, **63**, 86 (1989).
11. I. Affleck, *Phys. Rev. Lett.*, **65**, 2477 (1990).
12. M. Takahashi, and T. Sakai, *J. Phys. Soc. Jpn.*, **60**, 760 (1991).
13. A. M. Tsvelik, *Phys. Rev. B*, **42**, 10499 (1990).
14. I. Affleck, *Phys. Rev. B*, **43**, 3215 (1991).
15. S. Sachdev, T. Senthil, and R. Shankar, *Phys. Rev. B*, **50**, 258 (1994).
16. A. Furusaki, and S.-C. Zhang, *Phys. Rev. B*, **60**, 1175 (1999).
17. V. Kiryukhin, and B. Keimer, *Phys. Rev. B*, **52** (1995).
18. H. Kageyama, K. Yoshimura, R. Stern, N. V. Mushnikov, K. Onizuka, M. Kato, K. Kosuge, C. P. Slichter, T. Goto, and Y. Ueda, *Phys. Rev. Lett.*, **82**, 3168 (1999).
19. K. O. et al., *J. Phys. Soc. Jpn.*, **69**, 1016 (2000).
20. C. Ruegg, N. Cavadini, A. Furrer, H.-U. Gudel, K. Kramer, H. Mutka, A. Wildes, K. Habicht, and P. Vorderwisch, *Nature*, **423**, 62 (2003).
21. K. Kodama, M. Takigawa, M. Horvatic, C. Berthier, H. Kageyama, Y. Ueda, S. Miyahara, F. Becca, and F. Mila, *Science*, **298**, 395 (2003).
22. J. P. Renard, M. Verdaguer, L. P. Regnault, W. A. C. Erkelens, J. Rossat-Mignod, and W. G. Stirling, *Europhys. Lett.*, **3**, 945 (1987).
23. S. Ma, C. Broholm, D. H. Reich, B. J. Sternlib, and R. W. Erwin, *Phys. Rev. Lett.*, **69**, 3571 (1992).
24. L.-P. Regnault, I. A. Zaliznyak, and S. V. Meshkov, *J. Phys.: Condens. Matter*, **5**, L677 (1993).
25. L. P. Regnault, I. Zaliznyak, J. P. Renard, and C. Vettier, *Phys. Rev. B*, **50**, 9174 (1994).
26. I. Zaliznyak, D. C. Dender, C. Broholm, and D. H. Reich, *Phys. Rev. B*, **57**, 5200 (1998).
27. M. Chiba, Y. Ajiro, H. Kikuchi, T. Kubo, and T. Morimoto, *Phys. Rev. B*, **44**, 2838 (1991).
28. P. P. Mitra, and B. I. Halperin, *Phys. Rev. Lett.*, **72**, 912 (1994).
29. Z. Honda, H. Asakawa, and K. Katsumata, *Phys. Rev. Lett.*, **81**, 2566 (1998).
30. Z. Honda, K. Katsumata, M. Hagiwara, and M. Tokunaga, *Phys. Rev. B*, **60**, 9272 (1999).
31. Y. Chen, Z. Honda, A. Zheludev, C. Broholm, K. Katsumata, and S. M. Shapiro, *Phys. Rev. Lett.*, **86**, 1618 (2001).
32. A. Zheludev, Y. C. Z. Honda, C. Broholm, and K. Katsumata, *Phys. Rev. Lett.*, **88**, 077206 (2002).
33. A. Zheludev, Z. Honda, C. Broholm, K. Katsumata, S. M. Shapiro, A. Kolezhuk, S. Park, and Y. Qiu, *Phys. Rev. B*, **68**, 134438 (2003).
34. M. Hagiwara, Z. Honda, K. Katsumata, A. K. Kolezhuk, and H.-J. Mikeska, *Phys. Rev. Lett.*, **91**, 177601 (2003).
35. A. Zheludev, S. M. Shapiro, Z. Honda, K. Katsumata, B. Grenier, E. Ressouche, L.-P. Regnault, Y. Chen, P. Vorderwisch, H.-J. Mikeska, and A. K. Kolezhuk, *Phys. Rev. B*, **69**, 054414 (2004).
36. A. Zheludev, B. Grenier, E. Ressouche, L.-P. Regnault, Z. Honda, and K. Katsumata, *Phys. Rev. B*, **71**, 104418 (2005).
37. Z. Honda, K. Katsumata, H. A. Katori, K. Yamada, T. Ohishi, T. Manabe, and M. Yamashita, *J. Phys.: Condens. Matter*, **9**, 3487 (1997).
38. A. Zheludev, Z. Honda, K. Katsumata, R. Feyerherm, and K. Prokes, *Europhys. Lett.*, **55**, 868 (2001).
39. Y. Narumi, M. Hagiwara, M. Kohno, and K. Kindo, *Phys. Rev. Lett.*, **86**, 324 (2001).
40. A. Zheludev, T. Masuda, B. Sales, D. Mandrus, T. Papenbrock, T. Barnes, and S. Park, *Phys. Rev. B*, **69**, 144417 (2004).
41. L. P. Regnault *et al.*, *Physica (Amsterdam)*, **66**, 350B (2004).
42. M. Hagiwara, L. P. Regnault, A. Zheludev, A. Stunault, N. Metoki, T. Suzuki, S. Suga, K. Kakurai, Y. Koike, P. Vorderwisch, , and J.-H. Chung, *Phys. Rev. Lett.*, **94**, 177202 (2005).
43. A. Zheludev, Y. Chen, C. Broholm, Z. Honda, and K. Katsumata, *Phys. Rev. B*, **63**, 104410 (2001).
44. O. Golinelli, T. Jolicoeur, and R. Lacaze, *J. Phys. Condens. Matter*, **5**, 1399 (1993).
45. S. V. Meshkov, *Phys. Rev. B*, **48**, 6167 (1993).
46. E. S. Sorensen, and I. Affleck, *Phys. Rev. B*, **49**, 15771 (1994).
47. T. Suzuki, and S. Suga, *Phys. Rev. B*, **68**, 134429 (2003).
48. P. C. Hohenberg, and W. F. Brinkman, *Phys. Rev. B*, **10**, 128 (74).
49. T. Suzuki, and S. Suga (2005), cond-mat/0505196.
50. T. Barnes, and J. Riera, *Phys. Rev. B*, **50**, 6817 (1994).
51. I. Affleck, and R. A. Weston, *Phys. Rev. B*, **45**, 4667 (1992).
52. F. H. L. Essler, *Phys. Rev. B*, **62**, 3264 (2000).
53. O. Golinelli, T. Jolicoeur, and R. Lacaze, *Phys. Rev. B*, **45**, 9798 (1992).
54. T. Sakai, *Phys. Rev. B*, **62**, R9240 (2000).
55. F. H. L. Essler, and I. Affleck, *J. Stat. Mech.*, p. P12006 (2004).
56. (2005), I.-P. Regngault, A. Zheludev, M. Hagiwara, A. Stunault, to be published.
57. Zaliznyak, M. Enderle, C. Broholm, L.-P. Regnault, D. Reich, J. Rittner, M. Sieling, K. Katsumata,

- P. Vorderwisch, and M. Meissner, unpublished.
58. T. Masuda, A. Zheludev, H. Manaka, and J.-H. Chung (2005), cond-mat/0506382.
 59. H. Manaka, I. Yamada, Z. Honda, H. A. Katori, and K. Katsumata, *J. Phys. Soc. Jpn.*, **67**, 3913 (1998).
 60. Y.-J. Wang, cond-mat/0306365 (2003).
 61. H. Tsujii, Z. Honda, B. Andraka, K. Katsumata, and Y. Takano, *Phys. Rev. B*, **71**, 014426 (2005).